Geophysical Journal International

Geophys. J. Int. (2010) doi: 10.1111/j.1365-246X.2010.04633.x

An explicit relationship between time-domain noise correlation and spatial autocorrelation (SPAC) results

Victor C. Tsai and Morgan P. Moschetti

Geologic Hazards Team, United States Geological Survey, Golden, CO 80401, *USA. E-mail: vtsai@post.harvard.edu*

Accepted 2010 April 18. Received 2010 April 7; in original form 2009 December 10

SUMMARY

The success of recent ambient noise tomographic studies is now understood to arise due to cross-correlation properties documented in the acoustics community since the 1950s. However, despite the fact that Aki's 1957 spatial autocorrelation (SPAC) work yields identical analytical results to certain noise correlation results, the precise relationship between SPAC and time-domain cross-correlation remains not entirely transparent. Here, we present an explicit comparison of the two approaches and clarify that SPAC theory is indeed equivalent to the cross-correlation theory used for recent noise tomography studies. This equivalence allows theoretical work from each field to be applied to the other, and we illustrate a few examples of this.

Key words: Surface waves and free oscillations; Seismic tomography; Theoretical seismology; Wave propagation; Crustal structure.

1 INTRODUCTION

Recent work, beginning with Campillo & Paul (2003), Shapiro & Campillo (2004) and Shapiro *et al.* (2005), has shown that it is possible to perform high-quality seismic tomography by taking time-domain cross-correlation measurements of the ambient seismic noise field. This procedure is now known as ambient noise tomography. These studies were originally motivated by results of Lobkis & Weaver (2001), which give a relationship between cross-correlation measurements and the Green's function under very restrictive conditions; however, the success of ambient noise tomography is now best understood to result from noise correlation properties determined by Eckart (1953), Aki (1957), Jacobson (1962) and Cox (1973), which can account for the known non-uniformity in the ambient seismic noise wavefield.

Despite the fact that Aki's application (Aki 1957, henceforth Aki) was the most similar to the recent noise tomography applications, his theoretical formulation is the most different, in that, he discusses spatial autocorrelation rather than time-domain cross correlation. The exact agreement between Aki's analytical results and those of Cox (1973) has led a number of authors (e.g. Chavez-Garcia & Luzon 2005; Chavez-Garcia *et al.* 2005; Nakahara 2006; Sanchez-Sesma & Campillo 2006; Ekström *et al.* 2009; Tsai 2009) to infer that the formulations are simply describing the same physics but with different language. However, an explicit relationship between the two theories has not yet been made. In this paper, we clearly provide this relationship, thus showing that indeed the theories can be reinterpreted as different formulations of the same theory. The explicit equivalence between the theories can then be used to apply theoretical work from each field to the other, without needing to reformulate the problem in terms of the other theory. We illustrate a few examples of applying known results from one field to the other field in which these results have not yet been widely appreciated.

2 DEFINITIONS OF TIME-DOMAIN CROSS CORRELATION AND SPATIAL AUTOCORRELATION

Time-domain cross correlation is a common tool used to find similarities between two different time-series and can be defined as

$$C_{fg}(t) \equiv \frac{1}{2T}\int_{-T}^{T} f(\tau)g(\tau + t)\mathrm{d}\tau, \tag{1}$$

where $f(t)$ and $g(t)$ are the original (real-valued) time-series, t is time, τ is integration time and C_{fg} is the normalized cross correlation over correlation time $2T$. In noise tomography applications, f and g are taken to be (e.g. vertical displacement) seismograms from two different locations and can therefore be written as $f(t) = u(\boldsymbol{x}_1, t)$, $g(t) = u(\boldsymbol{x}_2, t)$, where $u(\boldsymbol{x}, t)$ is the seismogram at spatial location $\boldsymbol{x}$, so that eq. (1) can be rewritten as

$$C_{x_1x_2}(t) \equiv \frac{1}{2T}\int_{-T}^{T} u(\boldsymbol{x}_1, \tau)u(\boldsymbol{x}_2, \tau + t)\mathrm{d}\tau. \tag{2}$$

On the other hand, spatial autocorrelation, also known as spatially averaged coherency (Asten 2006), is used to find similarities in a spatial field and can be defined as

$$\phi(\boldsymbol{\xi}) \equiv \frac{1}{A}\int_{A} F(\boldsymbol{x})F(\boldsymbol{x} + \boldsymbol{\xi})\mathrm{d}\boldsymbol{x}, \tag{3}$$

where F is a (real-valued) field over the spatial variable $\boldsymbol{x}$, $\boldsymbol{x}$ takes on values from the region (or area) A, $\boldsymbol{\xi}$ is also a spatial variable and ϕ is the normalized spatial autocorrelation (SPAC). As applied

by Aki to a seismic wavefield, then $F(\boldsymbol{x}) = u(\boldsymbol{x}, t)$ also has a time dependence and so eq. (3) can be rewritten as

$$\phi(\boldsymbol{\xi}, t) \equiv \frac{1}{A}\int_A u(\boldsymbol{x}, t)u(\boldsymbol{x}+\boldsymbol{\xi}, t)\mathrm{d}\boldsymbol{x}, \tag{4}$$

where Aki interprets $\boldsymbol{x}$ as a stochastic random variable and is therefore integrated over an ensemble A (rather than $\boldsymbol{x}$ being averaged over a spatial area A, as is more common for spatial autocorrelation), and A denotes both the ensemble itself and the size of the ensemble. In practice, a lengthy time-series is taken as a proxy of an ensemble, and this average is then taken over time t (with $-T < t < T$) rather than over ensemble A (with $\boldsymbol{x} \in A$).

3 SUMMARY OF BOTH THEORIES

To make an explicit comparison between the time-domain cross-correlation theory and the spatial autocorrelation theory, it is useful to summarize the results of each. The results shown in Section 3 are not new, and are expected to be known by the respective communities, but are useful to present in parallel. In the following, we have taken the approach of Tsai (2009) to describe both results. This simple approach most easily allows for a direct and transparent comparison between the two results. Although this approach may not be as rigorous as, for example, Cox (1973) and Capon (1973), the clarity obtained from the results of this approach may not be as easily obtained with those other approaches. The approach inherently relies on the existence of uncorrelated 'noise' sources, but allows for these noise sources to be distributed non-uniformly in space, therefore not necessarily satisfying the assumptions of equipartition or noise-source isotropy of some other noise correlation studies (e.g. Lobkis & Weaver 2001; Wapenaar 2004; Sanchez-Sesma & Campillo 2006; Wapenaar & Fokkema 2006).

Because the vast majority of ambient noise tomography applications (e.g. Sabra *et al.* 2005; Yao *et al.* 2006; Lin *et al.* 2008) and SPAC applications (e.g. Köhler *et al.* 2007; Stephenson *et al.* 2009) have focused on analysing direct-arrival surface waves, we discuss the theories only as they relate to potentially dispersive waves travelling in two dimensions (2D, with the third dimension being integrated out), without attenuation. It may be noted that both theories discussed below can be generalized to the case of observing multiple (attenuating) phase arrivals, including body waves and any other arrivals (e.g. coda) that may be expected (e.g. Aki 1957; Tsai 2009), but that the pre-dominance of direct surface waves makes it difficult to observe these phases in practice. The formulations discussed later are appropriate for both Rayleigh and Love waves as long as one is careful in treating source densities, with polarizations included properly, as in Aki (1957).

3.1 Noise cross-correlation theory

It was first observed by Jacobson (1962) (and later confirmed by Cox 1973, and many others) that for isotropic noise of a single frequency, ω,

$$C_{x_1x_2}(t, \omega) \equiv C_{x_1x_2}(t) = J_0(\omega r/c)\cdot\cos(\omega t), \tag{5}$$

where J_0 is a Bessel function of order zero, r is the distance between $\boldsymbol{x}_1$ and $\boldsymbol{x}_2$ and c is the velocity of the waves. In this theory, it is assumed that the noise field is isotropic in the sense that the waves are generated by a uniformly distributed set of noise generators equally spaced along a circle infinitely far from the two stations.

As shown by Tsai (2009), this result can be obtained in the following simple manner. First, the case of a deterministic wave source of frequency ω is examined. For this case, then $u(\boldsymbol{x}_k, t) = \cos[\omega(t - t_k)]$, and it is observed that $C_{x_1x_2}$ (as defined by eq. 2) is given by

$$\begin{aligned} C_{x_1x_2}(t, \omega) &= \frac{1}{2T}\int_{-T}^{T}\cos[\omega(\tau - t_1)]\cos[\omega(\tau + t - t_2)]\mathrm{d}\tau \\ &= \frac{1}{2}\cos[\omega(t - \Delta t)] \\ &\quad - \frac{\sin[2\omega T]}{4\omega T}\cos[\omega(t - \Delta t) - 2\omega t_1] \\ &\approx \frac{1}{2}\cos[\omega(t - \Delta t)], \end{aligned} \tag{6}$$

where $\Delta t \equiv t_2 - t_1$ is the time delay between waves arriving at $\boldsymbol{x}_1$ and $\boldsymbol{x}_2$. The last approximation is valid as long as $T \gg 1/\omega$, that is the correlation time T is sufficiently long, and holds for arbitrary phase shift ωt_1. An expression for Δt is easily obtained by considering the geometry of the problem and is given by $\Delta t = r\cos\theta/c$ for direct-arrival far-field surface waves in a homogeneous velocity medium, where r is the distance between $\boldsymbol{x}_1$ and $\boldsymbol{x}_2$, θ is the azimuth of the source relative to the station–station line and c is the velocity of the wave. All solutions derived below (e.g. eq. 5, with Bessel function dependence) are for this simple form of Δt. Body-wave or coda arrivals in a potentially heterogeneous medium could be described by using an appropriately modified expression for Δt, and would result in modified solutions.

At this point, we observe that given uncorrelated 'noise' sources (including scattering sources) at all different azimuths, the assumption that these sources are uncorrelated (with random phases) implies that cross-term contributions to $C_{x_1x_2}$ cancel and we are simply left with a sum of terms like in eq. (6). With a distribution of sources that is continuous, then

$$\begin{aligned} C_{x_1x_2}(t, \omega) &= \int_0^{2\pi}\rho_S(\theta, \omega)\cos[\omega(t - r\cos\theta/c)]\,\mathrm{d}\theta \\ &= Re\left[\mathrm{e}^{\mathrm{i}\omega t}\int_0^{2\pi}\rho_S(\theta, \omega)\mathrm{e}^{-\mathrm{i}\omega r\cos\theta/c}\mathrm{d}\theta\right], \end{aligned} \tag{7}$$

where $\rho_S(\theta, \omega)$ is the density of noise sources as a function of azimuth θ at the given frequency ω. If only data in a specified time window are used (as is common in noise tomography approaches), one must down-weight the contribution to ρ_S from those times t corresponding to those azimuths θ contributing to eq. (7) (Tsai 2009). This important point will be discussed in more detail in Section 4.2. For the time being, it is assumed that no windowing is done. In Section 4.2, it will be seen that applying a time window can, in some cases, be very useful. We further note that for horizontally polarized waves (e.g. horizontal component Rayleigh and Love waves), ρ_S must include the polarization dependence so that, for example, a uniform distribution of incident Love waves would give ρ_S with a $\sin^2\theta$ or $\cos^2\theta$ dependence (Aki 1957).

A constant density of sources in azimuth (with no time windowing and no polarization) implies ρ_S is constant with respect to azimuth θ, but potentially has a dependence on frequency. We can then write $\rho_S = \Phi(\omega)$, where $\Phi(\omega)$ is the strength of the source at frequency ω (i.e. Φ is the spectral density, as in Cox 1973). Evaluating eq. (7) then yields

$$\begin{aligned} C_{x_1x_2}(t, \omega) &= Re\left[\mathrm{e}^{\mathrm{i}\omega t}\int_0^{2\pi}\Phi(\omega)\mathrm{e}^{-\mathrm{i}\omega r\cos\theta/c}\mathrm{d}\theta\right] \\ &= Re\left[\{\mathrm{e}^{\mathrm{i}\omega t}\cdot\Phi(\omega)\cdot 2\pi J_0(\omega r/c)\right] \\ &= 2\pi\,\Phi(\omega)\cdot J_0(\omega r/c)\cdot\cos(\omega t). \end{aligned} \tag{8}$$

At this point, we note that the source strength (or spectral density) $\Phi(\omega)$ can be determined by observations of Φ at either $\boldsymbol{x}_1$ or $\boldsymbol{x}_2$. For a time-series with sources at multiple frequencies, Φ is given by

$$\Phi(\boldsymbol{x}_k, \omega) \equiv \frac{|\mathbb{F}[u(\boldsymbol{x}_k, t)]|^2}{2\pi}, \tag{9}$$

where $\mathbb{F}$ denotes the Fourier transform. We therefore observe that if $u(\boldsymbol{x}_k, t)$ is pre-whitened prior to cross correlation so that

$$\tilde{u}(\boldsymbol{x}_k, t) = \mathbb{F}^{-1}\left[\frac{\mathbb{F}[u(\boldsymbol{x}_k, t)]}{|\mathbb{F}[u(\boldsymbol{x}_k, t]|}\right], \tag{10}$$

where $u(\boldsymbol{x}_k, t)$ is the original time-series and $\tilde{u}(\boldsymbol{x}_k, t)$ is the pre-whitened time-series, then $\Phi(\omega) = 1/2\pi$ for $\tilde{u}(\boldsymbol{x}_k, t)$ so that

$$\begin{aligned}\tilde{C}_{x_1x_2}(t, \omega) &\equiv \frac{1}{2T}\int_{-T}^{T} \tilde{u}(\boldsymbol{x}_1, \tau)\tilde{u}(\boldsymbol{x}_2, \tau + t)\mathrm{d}\tau \\ &= J_0(\omega r/c) \cdot \cos(\omega t),\end{aligned} \tag{11}$$

and we recover eq. (5), the result of Jacobson (1962).

3.2 SPAC theory

In Aki's original 1957 theory, the assumption made is that the wavefield is stationary in both space and time so that the energy in different modes is equipartitioned. A similar assumption was taken by Lobkis & Weaver (2001). The result of this assumption is that the SPAC function $\phi(\boldsymbol{\xi}, t)$ is found to be independent of time t. However, it is well understood that if one actually calculates $\phi(\boldsymbol{\xi}, t)$, it is far from constant and only achieves an approximately constant value after averaging over a substantial time. In Aki's framework, this time averaging takes the place of ensemble averaging and so the ϕ actually discussed can be expressed as

$$\phi(\boldsymbol{\xi}) \equiv \frac{1}{2T}\int_{-T}^{T} u(\boldsymbol{x}, t)u(\boldsymbol{x} + \boldsymbol{\xi}, t)\mathrm{d}t. \tag{12}$$

Aki further introduces the notation

$$\bar{\phi}(r) \equiv \frac{1}{2\pi}\int_{|\boldsymbol{\xi}|=r} \phi(\boldsymbol{\xi})\mathrm{d}\boldsymbol{\xi} = \frac{1}{2\pi}\int_0^{2\pi} \phi(|\boldsymbol{\xi}| = r)\,\mathrm{d}\theta, \tag{13}$$

where θ is azimuth and $\bar{\phi}(r)$ is an azimuthal average of $\phi(\boldsymbol{\xi})$ over all $|\boldsymbol{\xi}| = r$. Aki also notes that this azimuthal average is equivalent to any individual $\phi(\boldsymbol{\xi})$ if noise sources are distributed uniformly in azimuth. Aki's final result is that for a single frequency, ω,

$$\bar{\rho}(r, \omega) \equiv \frac{\bar{\phi}(r, \omega)}{\phi(0, \omega)} = J_0(\omega r/c). \tag{14}$$

To facilitate comparison between the two different theories, we instead take the assumption as in Section 3.1 that the wavefield consists of plane waves arriving stochastically from different azimuths. This assumption was made by others (e.g. Capon 1973; Asten 1976) who also derive eq. (14). These authors also prefer to call $\phi(\boldsymbol{\xi})$ the spatial covariance rather than SPAC, and call $\bar{\rho}(r)$ the averaged coherency. These plane wave studies also clarify that equipartition need not be strictly satisfied, especially when comparing energies across different frequencies (rather than within a given narrow band of frequencies).

Again considering a single deterministic wave of frequency ω, $u(\boldsymbol{x}_k, t) = \cos[\omega(t - t_k)]$, we observe that $\phi(\boldsymbol{\xi}, \omega)$ (as defined by eq. 12) is given by

$$\begin{aligned}\phi(\boldsymbol{\xi}, \omega) &= \frac{1}{2T}\int_{-T}^{T} \cos[\omega(t - t_1)]\cos[\omega(t - t_2)]\mathrm{d}t \\ &= \frac{1}{2}\cos(\omega\Delta t) + \frac{\sin[2\omega T]}{4\omega T}\cos[\omega(t_1 + t_2)] \\ &\approx \frac{1}{2}\cos(\omega\Delta t) \;=\; \frac{1}{2}\cos(\omega r\cos\theta/c),\end{aligned} \tag{15}$$

where, as in eq. (6), we have used $\Delta t \equiv t_2 - t_1 = r\,\cos\theta/c$ and taken the approximation $T \gg 1/\omega$.

Again, as before, the assumption of uncorrelated noise sources (with random phases) implies that cross-term contributions to $\phi(\boldsymbol{\xi}, \omega)$ cancel and the result for noise sources at all different azimuths is

$$\begin{aligned}\phi(\boldsymbol{\xi}, \omega) &= \int_0^{2\pi} \rho_S(\theta, \omega)\cos(\omega r\cos\theta/c)\mathrm{d}\theta \\ &= Re\left[\int_0^{2\pi} \rho_S(\theta, \omega)\mathrm{e}^{\mathrm{i}\omega r\cos\theta/c}\mathrm{d}\theta\right],\end{aligned} \tag{16}$$

where $\rho_S(\theta, \omega)$ is again the density of sources as a function of azimuth θ at the given frequency ω.

At this point, we observe that if ρ_S is uniform in azimuth then $\rho_S(\theta, \omega) = \Phi(\omega)$ and we immediately find

$$\begin{aligned}\phi(\boldsymbol{\xi}, \omega) &= Re\left[\int_0^{2\pi} \Phi(\omega)\mathrm{e}^{\mathrm{i}\omega r\cos\theta/c}\mathrm{d}\theta\right] \\ &= 2\pi\,\Phi(\omega)J_0(\omega r/c).\end{aligned} \tag{17}$$

On the other hand, if $\rho_S(\theta, \omega) = \rho_S(\theta)\Phi(\omega)$, then regardless of $\rho_S(\theta)$ the azimuthal average $\bar{\phi}(r)$ is given by

$$\begin{aligned}\bar{\phi}(r, \omega) &= \frac{1}{2\pi}\int_0^{2\pi} Re\left[\int_0^{2\pi} \rho_S(\theta - \theta_2)\Phi(\omega)\mathrm{e}^{\mathrm{i}\omega r\cos\theta/c}\mathrm{d}\theta\right]\mathrm{d}\theta_2 \\ &= \frac{\Phi(\omega)}{2\pi}Re\left[\int_0^{2\pi}\left(\int_0^{2\pi} \rho_S(\theta - \theta_2)\mathrm{d}\theta_2\right)\mathrm{e}^{\mathrm{i}\omega r\cos\theta/c}\mathrm{d}\theta\right] \\ &= \frac{\Phi(\omega)}{2\pi}Re\left[\int_0^{2\pi} 2\pi\cdot\mathrm{e}^{\mathrm{i}\omega r\cos\theta/c}\mathrm{d}\theta\right] \\ &= 2\pi\,\Phi(\omega)J_0(\omega r/c).\end{aligned} \tag{18}$$

In simplifying this expression, the order of integration on θ and θ_2 has been changed and we assume a normalization on $\rho_S(\theta)$ such that

$$\frac{1}{2\pi}\int_0^{2\pi} \rho_S(\theta)\mathrm{d}\theta = 1. \tag{19}$$

Comparing eq. (17) with eq. (18), we have a simple proof of the equivalence between an azimuthal average and uniformly distributed noise sources.

Substituting this expression into $\bar{\rho}(r, \omega) = \bar{\phi}(r, \omega)/\phi(0, \omega)$ then yields

$$\bar{\rho}(r, \omega) = \frac{2\pi\,\Phi(\omega)J_0(\omega r/c)}{2\pi\,\Phi(\omega)\cdot 1} = J_0(\omega r/c), \tag{20}$$

and we recover eq. (14), the result of Aki (1957).

4 COMPARISON OF CROSS CORRELATION AND SPAC RESULTS

4.1 Equivalence of $\phi(r, \omega)$ and $C_{x_1x_2}(0, \omega)$

Comparison of eq. (2) and eq. (12) shows that eq. (12) is a special case of eq. (2). Letting $\boldsymbol{x} = \boldsymbol{x}_1$, $\boldsymbol{x} + \boldsymbol{\xi} = \boldsymbol{x}_2$, it is clear that

$$\phi(\boldsymbol{\xi}) \equiv C_{x_1x_2}(0) \tag{21}$$

so that $\phi(\boldsymbol{\xi})$ is simply a special case of $C_{x_1x_2}(t)$. That is, the SPAC [as defined by eq. (12), and as is used by the SPAC community] is the value of the bandpassed cross correlation at zero time lag ($t = 0$). This fact is not surprising, and is also suggested by Cox (1973), but is not immediately obvious from the original definition of SPAC in eq. (4). The equivalence thus obviates the many strong similarities in the derivations of Section 3.1 and Section 3.2. For example, eqs (15)–(17) are special cases of eqs (6)–(8). However, if the azimuthal average of eq. (18) is applied, then the methods diverge slightly; this average, for example, will only yield a single (averaged) velocity measurement from an array of stations whereas each pair of stations can theoretically yield independent measurements (if the noise source distribution is close enough to uniform).

One may also note that SPAC processing requires filtering into Fourier components prior to applying eq. (12), which then amounts to multiplication in the frequency domain (along with complex conjugation of one term). Since cross correlation in the time-domain is equivalent to this multiplication in the frequency domain, this is another way of understanding the equivalence of the theories. This fact has also been pointed out by Chavez-Garcia *et al.* (2005) and used by Ekström *et al.* (2009). Asten (2006) and Nakahara (2006) also point out that Aki's SPAC is similar to 'coherency', that is, cross correlation in the frequency domain. A comparison of the results in the frequency domain is therefore useful. First, we define

$$f \equiv Re[f] + i\,\mathrm{Im}[f] \equiv \int_0^{2\pi} \rho_S(\theta, \omega) \mathrm{e}^{\mathrm{i}\omega r \cos\theta/c} \mathrm{d}\theta, \tag{22}$$

so that $\phi(\boldsymbol{\xi}, \omega) = Re[f]$ and $C_{x_1x_2}(t, \omega) = Re[\mathrm{e}^{-\mathrm{i}\omega t} f]$. Taking the Fourier transform of $C_{x_1x_2}(t, \omega)$ then yields

$$\begin{aligned}\mathbb{F}[C_{x_1x_2}(t, \omega_0)] = {} & \pi(Re[f] - i\,\mathrm{Im}[f])\delta(\omega - \omega_0) \\ & + \pi(Re[f] + i\,\mathrm{Im}[f])\delta(\omega + \omega_0).\end{aligned} \tag{23}$$

It is therefore seen that $\phi(\boldsymbol{\xi}, \omega_0)$ is the real part of the cross-correlation spectrum (i.e. 'coherency') at frequency $\omega = \omega_0$ (up to a constant that depends on choice of Fourier transform normalization convention). Eq. (23) also points out the possibility of using the imaginary part of the spectrum, as is common in noise tomography applications (e.g. Bensen *et al.* 2007, who use phase measurements) and has been done in some SPAC applications as well (e.g. Asten 2006).

4.2 Applying results of one theory to the other

The usefulness of drawing the connection between the two sets of theories is that theoretical results from each field, which have so far remained fairly separate and not used by the other scientific community, can be applied to the other. For example, there has been a large amount of theoretical work done in the SPAC field since the results of Aki (1957), including Capon (1973), Asten (1976), Henstridge (1979), Cho *et al.* (2004) and Asten (2006). On the other hand, there has also been some fairly recent theoretical work done to understand the results of noise tomography, including Snieder (2004) and Tsai (2009). Here, we illustrate just a few examples of applying well-known results in one field to the other. It is expected that there are other applications beyond the ones listed.

4.2.1 Azimuthal averaging

The first obvious application is applying eq. (18) to cross-correlation results. That is, the same azimuthal averaging technique performed in eq. (18) can be applied generally to $C_{x_1x_2}(t, \omega)$ to show that

$$\bar{C}_{x_1x_2}(t, \omega) = 2\pi\,\Phi(\omega)\,J_0(\omega r/c)\,\cos(\omega t), \tag{24}$$

where $\bar{C}_{x_1x_2}$ is an azimuthal average as in eq. (13). Thus, if cross-correlation measurements in a certain region are made for a range of different azimuths, the assumption of isotropic noise sources is no longer needed, and instead one only needs to consider the difficulties inherent in the SPAC approach (e.g. the need to correct for uneven station spacing if the stations are not equally spaced). This method can be used, for example, to make more accurate noise tomography measurements when station spacing is small (relative to the relevant wavelength), a regime known to sometimes produce inaccurate results with standard processing techniques (and for which data are sometimes therefore unused). This explicit averaging should provide more accurate results than if one does not use the averaging and instead simply assumes that the averaging of ray paths accounts for the non-uniformity of noise sources.

One complication that arises when performing this averaging for noise tomography applications is that the coherent noise (with non-random phases) contributing to a meaningful measurement is typically a small fraction of the total noise level. When performing the whitening of eq. (10), then, one should whiten with respect to the coherent noise level rather than the total noise level. This coherent noise level is difficult to determine, but can be estimated in the following way. First, we assume that the fraction of coherent noise is $\chi(\omega)$ in each of the N cross correlations to be stacked. If whitening is done with respect to the total noise level, instead of the coherent noise level, then the stacked signal will have coherent amplitude $N\chi$ (increasing linearly) and incoherent amplitude $R_w(1-\chi) \sim \sqrt{N}(1-\chi)$, where R_w is the expectation of a random walk. Assuming a uniform noise distribution then the stacked signal will be $N\,\chi[\omega)J_0(\omega r/c) + \sqrt{N}(1 - \chi(\omega)]U_{wn}(\omega)$, where $U_{wn}(\omega)$ is a unit amplitude white noise spectrum. One can then estimate χ by taking the ratio of the J_0 amplitude to the U_{wn} amplitude and use this estimate to calculate a 'coherent' whitening using $\chi(\omega)$ for additional normalization. The $\chi(\omega)$ obtained in this way can also be used to infer characteristics of the ambient noise field.

4.2.2 Application at $\lambda \ll r$

Snieder (2004) and Tsai (2009) have both shown that noise tomography measurements (using cross-correlation techniques on single pairs of stations) generally accurately measure phase velocities in the regime when $\lambda \ll r$ where $\lambda = 2\pi c/\omega$ is the wavelength of the wave considered (equivalent to $\omega \gg c/r$). The assumptions made, for example by Tsai (2009), to obtain this result are that $\rho_S(\theta)$ is never zero (but can be arbitrarily small as long as one can go to arbitrarily small λ) and that severe velocity anomalies (strong velocity gradients) do not exist in the region. Even when these assumptions are not strictly respected, the errors are mostly less than a few per cent for relatively small λ/r. This result is counter to the common assumption in the SPAC community that SPAC techniques can only be used in the range $2 \lesssim \lambda/r \lesssim 15.7$ (Henstridge 1979; Chavez-Garcia *et al.* 2005). One reason for this apparent disparity is that traditional SPAC approaches rely on large enough azimuthal coverage for the full wavefield to be effectively uniformly sampled whereas traditional noise tomography approaches rely on a small enough azimuthal coverage that the wavefield observed is effectively uniform (over the azimuth range that the measurement is sensitive to). As shown with USArray data in Section 4.2.5 (with a distribution of noise that is uniform enough), these presumed different ranges of applicability can overlap, yielding good measurements

over the entire range of λ/r with both approaches. Results like those of Cox (1973), Tsai (2009) or Weaver *et al.* (2009) can be used to estimate the errors that arise (for a single pair measurement) when λ/r is non-zero, and results like those of Asten (2006) can be used to estimate errors for azimuthal averages. These errors are complementary in that the errors approach zero (independent of the distribution of noise sources) for opposite limits of λ/r ($\rightarrow 0$ versus $\rightarrow \infty$, respectively).

4.2.3 Use of windowing functions

Results for noise tomography measurements are also known to be sensitive to the choice of windowing function used (Tsai 2009). As an example of windowing, after cross correlations are made, it is standard practice in the noise tomography field to zero out the data at times of the cross correlations that are not expected to contribute to the desired velocity measurement (Bensen *et al.* 2007). In most applications, for example, arrivals at negative and positive time are separated by a significant amount of time. The time windowing then allows accurate measurements to be made even when significant noise (or signal not of interest) exists in the time duration between expected arrivals. This 'picking' of arrival windows when approximate arrival times are known can dramatically increase the signal-to-noise ratio and is partially responsible for the recent successes of ambient noise tomography. SPAC applications could also benefit from this type of time windowing. As shown by Tsai (2009), a windowed cross-correlation measurement with window $W(t)$ can be expressed as

$$C_{x_1x_2}(t,\omega) = Re\left[e^{i\omega t}\int W(\tau)\rho_S(\theta(\tau))\left|\frac{d\theta(\tau)}{d\tau}\right|e^{-i\omega\tau}d\tau\right]. \quad (25)$$

As also shown by Tsai (2009), when a strictly positive window function is used [$W(t) = H(t)$ where $H(t)$ is the Heaviside step function] with an isotropic distribution of noise (and a uniform velocity medium) then

$$\tilde{C}_{x_1x_2}(t,\omega) = \frac{1}{2}Re\left[e^{i\omega t}\left[J_0(\omega r/c) - iH_0(\omega r/c)\right]\right], \quad (26)$$

where H_0 is a Struve function of order zero, from which phase measurements are easily made. For this special case of window function

$$\phi(\boldsymbol{\xi},\omega) = \frac{1}{2}Re\left[J_0(\omega r/c) - iH_0(\omega r/c)\right] = \frac{1}{2}J_0(\omega r/c), \quad (27)$$

and it is seen that $\phi(\boldsymbol{\xi},\omega)$ is unaffected except for a normalization constant. This type of windowing may therefore be useful in certain SPAC applications where complete azimuthal coverage is not possible or when λ/r is relatively small. For example, utilizing a small enough time window around the expected arrival times would allow otherwise standard SPAC processing to obtain good measurements for λ/r well outside the range discussed in Section 4.2.2

4.2.4 Positive and negative signals of different amplitude

Generalizing the previous result, we consider the case of $W(t)\rho_S[\theta(t)] = \alpha + (\beta - \alpha)H(t)$ so that the field measured is a uniform distribution of noise at negative delay times (of amplitude α) plus a uniform distribution of noise at positive delay times of a different amplitude (β). Using this $W(t)\rho_S[\theta(t)]$ in eq. (25) then

$$C_{x_1x_2}(t,\omega) = \frac{1}{2}Re\left[e^{i\omega t}\cdot\left[(\beta+\alpha)J_0(\omega r/c) - i(\beta-\alpha)H_0(\omega r/c)\right]\right], \quad (28)$$

and

$$\phi(\boldsymbol{\xi},\omega) = \frac{1}{2}Re\left[(\beta+\alpha)J_0(\omega r/c) - i(\beta-\alpha)H_0(\omega r/c)\right] = \frac{\alpha+\beta}{2}J_0(\omega r/c), \quad (29)$$

again showing that for this special combination of $W(t)\rho_S[\theta(t)]$, the SPAC is unaffected except for a normalization constant. Eq. (29) therefore explains why it is possible to retrieve a meaningful velocity measurement (Ekström *et al.* 2009) even when the noise distribution is far from uniform (and without windowing the data). When the primary non-uniformity in the noise distribution is simply a difference between the positive and negative arrivals, and is otherwise 'effectively uniform', then the real part of the cross-correlation spectrum [i.e. $\phi(\boldsymbol{\xi},\omega)$] is still given by the same expression as for completely uniform noise (except for renormalization), and only the imaginary part of the spectrum is modified. As is clear from the results of Tsai (2009), 'effectively uniform' in this context means uniform in an azimuthal range covering the station–station line that corresponds to a cross-correlation time delay range $\Delta t \gg 1/\omega$. Eq. (28) also shows that if this situation exists, the imaginary part of the spectrum [$H_0(\omega r/c)$ up to normalization] can be used to yield a second velocity measurement.

Alternatively, one can follow the approach of Cox (1973), and expand $W[t(\theta)]\rho_S(\theta)$ as a Fourier series. To first order, we can write $W[t(\theta)]\rho_S(\theta) \approx \alpha' + \beta'\cos(\theta) + \gamma'\sin(\theta)$ and inserting into eq. (25) yields

$$C_{x_1x_2}(t,\omega) = \frac{1}{2}Re\left[e^{i\omega t}\cdot\left[\alpha' J_0(\omega r/c) - i\beta' J_1(\omega r/c)\right]\right], \quad (30)$$

and

$$\phi(\boldsymbol{\xi},\omega) = \frac{1}{2}Re\left[\alpha' J_0(\omega r/c) - i\beta' J_1(\omega r/c)\right] = \frac{\alpha'}{2}J_0(\omega r/c), \quad (31)$$

where J_1 is a Bessel function of order one. The similarity of $H_0(x)$ and $J_1(x)$ (they are similar at all x and asymptotically equivalent as $x \rightarrow \infty$) shows that the assumption of uniform noise from negative and positive delay times is nearly the same as using only the first term of a Fourier expansion (with correspondence $\alpha' \approx \beta + \alpha$, $\beta' \approx \beta - \alpha$).

4.2.5 Application to USArray Data

As proof of concept of some of the methods discussed in this section, we apply the methods to data from a set of four STS-2 USArray stations in central Nevada (TA.Q10A, TA.Q11A, TA.R10A and TA.R11A) that lie approximately in a square with sides of length 60 km. Standard processing was done to obtain cross correlations (Bensen *et al.* 2007), with day-long seismic records first being normalized in the time-domain with a running absolute mean and then whitened in the frequency domain with respect to the total noise level prior to cross correlation. The individual day cross correlations are then stacked, and the spectra for stacks of about 320 d of data are shown in Fig. 1. Since these spectra are not properly normalized for SPAC analysis, the amplitudes are influenced by noise source strength [$\Phi(\omega)$] but the zero crossings of the curves can still be

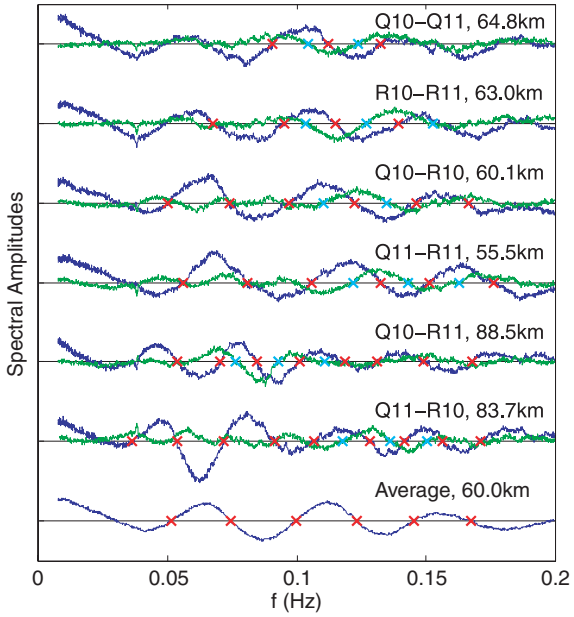

Figure 1. Raw cross-correlation spectra from six USArray station pairs in central Nevada. Blue curves are the real part of the spectra and green curves are the imaginary part. The crosses denote measured zero crossings, for the real (red) and imaginary (cyan) curves. The seventh plot is an azimuthal average of the six individual spectra, with frequencies normalized to a station–station spacing of 60 km. An azimuthal average of the imaginary part of the spectra is identically equal to zero and is not plotted.

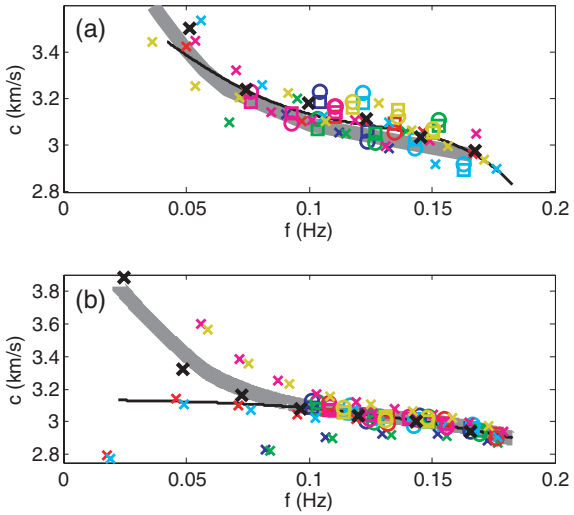

Figure 2. (a) Phase velocities measured from Fig. 1. Measurements for station pairs Q10–Q11 are blue, R10–R11 are green, Q10–R10 are red, Q11–R11 are cyan, Q10–R11 are magenta, Q11–R10 are yellow and azimuthal averages are black. Crosses are fit to J_0 (real part of spectra), circles are fit to H_0 (imaginary part) and squares are fit to J_1 (imaginary part). The thin black line is a fourth-degree polynomial fit to the measurements (not including the averages). The thick grey line is the approximate range of dispersion curves of Lin *et al.* (2008) for the same region. (b) Synthetic phase velocity measurements for the same station geometry, an arbitrary (non-uniform) noise distribution and using the average dispersion curve of Lin *et al.* (2008) as truth. Symbols are the same as in (a). As shown, the azimuthal averages (black crosses) perform better than the average curve (black line) at low frequencies. A few measurements plot off scale.

fit to those of J_0 (for the real part) and either H_0 or J_1 (for the imaginary part) as in Section 4.2.4 Fits to zero crossings of J_0 have been done previously by Aki (1957) and Ekström *et al.* (2009). In our example, no ambiguity exists in associating measured zero crossings with J_0 zeros because the data are well behaved for a range of frequencies that includes the first 7–10 zero crossings. (As an alternative to the zero-crossing measurement, one could co-estimate spectral amplitudes and phase velocities at all frequencies.)

Measuring phase velocities only at the zero crossings, we obtain the phase velocities shown in Fig. 2(a) (in the range $0.2 \leq \lambda/r \leq 1.1$). Only clearly identifiable zero crossings in frequency ranges with relatively large amplitudes are used. (The imaginary parts of the spectra are only large when the noise is very one-sided, resulting in many fewer measurements. It is also currently unclear whether H_0 or J_1 provide better approximations to the true situation.) In frequency ranges where amplitudes are low, measurements are easily biased due to spectral leakage from adjacent frequencies since each sinusoid of frequency ω (e.g. of eq. 6) contributing to the cross correlation (e.g. eq. 7) is actually tapered in time, giving contributions to the spectrum at frequencies other than ω. For example, measurements at $0.02 < f < 0.04$ Hz suffer from this problem (ambient noise levels are much higher at both higher and lower frequencies) and therefore are not used. A best-fit phase velocity dispersion curve is plotted through these measurements (in Fig. 2a) and agrees fairly well with the dispersion curves from central Nevada of Lin *et al.* (2008). We note that group velocity measurements could also have been made (including on the azimuthal average) if the data were all transformed back to the time-domain, but that the relatively short distance spacing of the stations used would likely result in large errors (Tsai 2009). We further note that some of the likely bias towards high phase velocities in the measurements (see Fig. 2a) is probably partially due to the assumption of uniform noise not being satisfied.

When the distribution of noise is very non-uniform, it may be useful to explicitly use the azimuthal averaging of Section 4.2.1, instead of averaging the individual dispersion measurements, since the two types of averaging can give different results. Unfortunately, when the distribution of noise is non-uniform, it becomes more difficult to estimate the proper normalization discussed in Section 4.2.1 since the real part of the individual spectra are no longer given exactly by J_0. We can, nonetheless, assume that the first-order differences in spectral amplitude are due to azimuthal variations and simply average the raw (not properly normalized) spectra. Accounting for station–station spacing differences by renormalizing frequencies by the station–station distance (relative to 60.0 km) prior to averaging, we obtain the azimuthal average curve shown in Fig. 1. Making phase velocity measurements from this curve results in the large black crosses in Fig. 2(a). Although these average measurements agree well with the dispersion curve calculated from averaging the individual measurements, synthetic tests (see Fig. 2b) suggest that the explicit azimuthal averaging can give better results when the distribution of noise is very non-uniform and when measurements are made at very low frequencies (e.g. around the first zero crossing of J_0).

5 CONCLUSIONS

In this work, we first summarize the theories for time-domain cross correlation of noise and for SPAC of noise. The exact equivalence between the cross correlation $C_{x_1x_2}$ (at $t = 0$) and the SPAC ϕ allows for an explicit relationship between the theories and allows results from each of the independent fields to be used in the other. A few examples are given of theoretical results that are understood in one of the fields but not widely appreciated in the other, and we explain

how these results can be applied. For example, we show how noise tomography can benefit from the azimuthal averaging of SPAC, and how SPAC can benefit from the time windowing common in noise tomography applications. The list of potential applications given is not meant to be comprehensive and it is expected that other useful connections will be found. This merger of the two fields therefore expands the methods available for application in each field and should reduce the amount of duplication of results that are already well known.

ACKNOWLEDGMENTS

The authors would like to thank S. Hartzell, M. W. Asten, W. J. Stephenson, F. C. Lin, R. Snieder and D. E. McNamara for helpful discussions, and two anonymous reviewers for helpful comments. Seismograms were provided by IRIS. This research was supported by the Mendenhall Postdoctoral Fellowship program of the United States Geological Survey.

REFERENCES

Aki, K., 1957. Space and time spectra of stationary stochastic waves, with special reference to microtremors, *Bull. Earthq. Res. Inst.,* **35,** 415–457.

Asten, M.W., 1976. The use of microseisms in geophysical exploration, *PhD thesis*, Macquarie University,Australia.

Asten, M.W., 2006. On bias and noise in passive seismic data from finite circular array data processed using SPAC methods, *Geophysics,* **71,** V153–V162.

Bensen, G.D., Ritzwoller, M.H., Barmin, M.P., Levshin, A.L., Lin, F., Moschetti, M.P., Shapiro, N.M. & Yang, Y., 2007. Processing seismic ambient noise data to obtain reliable broad-band surface wave dispersion measurements, *Geophys. J. Int.,* **169,** 1239–1260.

Campillo, M. & Paul, A., 2003. Long-range correlations in the diffuse seismic coda, *Science,* **299,** 547–549.

Capon, J., 1973. Signal processing and frequency-wavenumber spectrum analysis for a large aperture seismic array, in *Methods in Computational Physics,* Vol. 13, ed. Bolt, B.A., Academic Press Inc, New York.

Chavez-Garcia, F.J. & Luzon, F., 2005. On the correlation of seismic microtremors, *J. geophys. Res.,* **110**, doi:10.1029/2005JB003671.

Chavez-Garcia, F.J., Rodriguez, M. & Stephenson, W.R., 2005. An alternative approach to the SPAC analysis of microtremors: exploiting stationarity of noise, *Bull. seism. Soc. Am.,* **95,** 277–293.

Cho, I., Tada, T. & Shinozaki, Y., 2004. A new method to determine phase velocities of Rayleigh waves from microseisms, *Geophysics,* **69,** 1535–1551.

Cox, H., 1973. Spatial correlation in arbitrary noise fields with application to ambient sea noise, *J. acoust. Soc. Am.,* **54,** 1289–1301.

Eckart, C., 1953. The theory of noise in continuous media, *J. acoust. Soc. Am.,* **25,** 195–199.

Ekström, G., Abers, G.A. & Webb, S.C., 2009. Determination of surface-wave phase velocities across USArray from noise and Aki's spectral formulation, *Geophys. Res. Lett.,* **36**, doi:10.1029/2009GL039131.

Henstridge, J.D., 1979. A signal processing method for circular arrays, *Geophysics,* **44,** 179–184.

Jacobson, M.J., 1962. Space-time correlation in spherical and circular noise fields, *J. acoust. Soc. Am.,* **34,** 971–978.

Köhler, A., Ohrnberger, M., Scherbaum, F., Wathelet, M. & Cornou, C., 2007. Assessing the reliability of the modified three-component spatial autocorrelation technique, *Geophys. J. Int.,* **168,** 779–796.

Lin, F.C., Moschetti, M.P. & Ritzwoller, M.H., 2008. Surface wave tomography of the western United States from ambient seismic noise: Rayleigh and Love wave phase velocity maps, *Geophys. J. Int.,* **173,** 281–298, doi:10.1111/j.1365-246X.2008.03720.x.

Lobkis, O.I. & Weaver, R.L., 2001. On the emergence of the Green's function in the correlations of a diffuse field, *J. acoust. Soc. Am.,* **110,** 3011–3017.

Nakahara, H., 2006. A systematic study of theoretical relations between spatial correlation and Green's function in one-, two- and three-dimensional random scalar wavefields, *Geophys. J. Int.,* **167,** 1097–1105.

Sabra, K.G., Gerstoft, P., Roux, P., Kuperman, W.A. & Fehler, M.C., 2005. Surface wave tomography from microseismcs in Southern California, *Geophys. Res. Lett.,* **32**, doi:10.1029/2005GL023155.

Sanchez-Sesma, F.J. & Campillo, M., 2006. Retrieval of the green's function from cross correlation: The canonical elastic problem, *Bull. seism. Soc. Am.,* **96,** 1182–1191.

Shapiro, N.M. & Campillo, M., 2004. Emergence of broadband Rayleigh waves from correlations of the ambient seismic noise, *Geophys. Res. Lett.,* **31**, doi:10.1029/2004GL019491.

Shapiro, N.M., Campillo, M., Stehly, L. & Ritzwoller, M.H., 2005. High-resolution surface-wave tomography from ambient seismic noise, *Science,* **307,** 1615–1618.

Snieder, R., 2004. Extracting the Green's function from the correlation of coda waves: a derivation based on stationary phase, *Phys. Rev. E,* **69,** 1–8.

Stephenson, W.J., Hartzell, S., Frankel, A.D., Asten, M., Carver, D.L. & Kim, W.Y., 2009. Site characterization for urban seismic hazards in lower Manhattan, New York City, from microtremor array analysis, *Geophys. Res. Lett.*, **36**, doi:10.1029/2008GL036444.

Tsai, V.C., 2009. On establishing the accuracy of noise tomography travel-time measurements in a realistic medium, *Geophys. J. Int.,* **178,** 1555–1564.

Wapenaar, K., 2004. Retrieving the elastodynamic Green's function of an arbitrary inhomogeneous medium by cross correlation, *Phys. Rev. Lett.,* **93,** 1–4.

Wapenaar, K. & Fokkema, J., 2006. Green's function representations for seismic interferometry, *Geophysics,* **71,** SI33–SI46.

Weaver, R., Froment, B. & Campillo, M., 2009. On the correlation of non-isotropically distributed ballistic scalar diffuse waves, *J. acoust. Soc. Am.,* **126,** 1817–1826.

Yao, H., van der Hilst, R.D. & de Hoop, M.V., 2006. Surface-wave array tomography in SE Tibet from ambient seismic noise and two-station analysis - I. phase velocity maps, *Geophys. J. Int.,* **166,** 732–744.